### ISBN
9789290929376



### Authors
Lovat, G
Burghignoli, P
Capolino, F
et al.



### Publication Date
2006-11-01

### DOI
10.1109/eucap.2006.4584719

# BANDWIDTH ANALYSIS OF HIGHLY-DIRECTIVE PLANAR RADIATORS BASED ON PARTIALLY-REFLECTING SURFACES

**Giampiero Lovat**[1], **Paolo Burghignoli**[2], **Filippo Capolino**[3], **and David R. Jackson**[4]

[1] *"La Sapienza" University of Rome, Department of Electrical Engineering, Via Eudossiana 18, 00184 Roma, Italy. Email: lovat@die.uniroma1.it*

[2] *"La Sapienza" University of Rome, Department of Electronic Engineering, Via Eudossiana 18, 00184 Roma, Italy. Email: burghignoli@die.uniroma1.it*

[3] *University of Siena, Department of Information Engineering, Via Roma 56, 53100 Siena, Italy. Email: capolino@dii.unisi.it*

[4] *University of Houston, Department of Electrical and Computer Engineering, Houston, Texas, 77204-4005. Email: djackson@uh.edu*

## ABSTRACT

In this work, bandwidth properties of planar leaky-wave antennas made of a grounded dielectric slab covered with a partially-reflecting surface are investigated. The partially-reflecting surface is described by an equivalent shunt susceptance. It is shown that, with respect to a constant frequency-independent susceptance, the antenna bandwidth is not reduced using a frequency-dependent model, except for very specific cases. With reference to passive lossless structures, numerical examples are provided that illustrate the attainable performance and confirm the theoretical analysis.

Key words: Leaky-wave antennas; partially-reflecting surfaces; electromagnetic-bandgap structures; Fabry-Perot cavity.

## 1. INTRODUCTION

Planar leaky-wave (LW) antennas offer various advantages with respect to other highly-directive radiating systems in terms of structural simplicity, cost effectiveness and compatibility with planar integration [1], [2]. In a uniform two-dimensional (2D) configuration, their operating principle consists of the excitation by a simple source (e.g., a horizontal infinitesimal electric or magnetic dipole) of a pair of cylindrical TE and TM leaky waves along a planar layered structure [3]. One of the simplest among such planar configurations is a grounded dielectric slab covered with a dielectric and/or metallic screen that partially shields it (a Partially-Reflecting Surface, PRS) [4]-[6]. Some examples of such PRSs that have been studied in the past in connection with LW antennas are shown in Fig. 1: a thin high-permittivity dielectric layer (Fig. 1(a)) [7], a stack of alternating high- and low-permittivity layers (Fig. 1(b)) [8], a periodic array of metallic patches (Fig. 1(c)) [9], or a conducting plate with a periodic array of slots (Fig. 1(d)) [10].

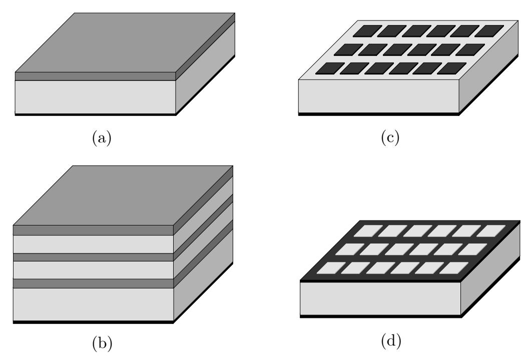


*Figure 1. Examples of LW antennas based on different types of PRS: (a) thin high-permittivity dielectric layer; (b) stack of alternating high- and low-permittivity layers; (c) periodic array of metallic patches; (d) periodic array of slots on a conducting plate.*

We consider here a PRS-covered grounded slab aimed at producing a narrow directive beam pointing at broadside, which can be used either as an antenna or as a screen for enhanced electromagnetic transmission through a subwavelength aperture. The analysis is based on a transverse equivalent representation of the structure under plane-wave incidence, in which the lossless PRS is modelled as a shunt susceptance (as shown in Fig. 2).

A study of this structure can be found in [6] where the PRS is represented by a constant, frequency-independent susceptance, while in [11] a LW interpretation of the main properties of the antenna for broadside radiation (i.e., gain, directivity, beamwidth, and bandwidth) is also provided. In particular, in these papers it is shown that the antenna is typically narrow-band when the PRS is repre-

*Proc. 'EuCAP 2006', Nice, France*
*6–10 November 2006 (ESA SP-626, October 2006)*

sented by a frequency-independent susceptance. However, it is not clear whether and how a more realistic *frequency-dependent* model of the PRS would lead to a deterioration of the bandwidth performance. In this study, simple inductors or capacitors are considered as PRS transverse models, along with series- and parallel-$LC$ circuits. In Sec. 2 previous analyses and findings are summarized. The main result of the present investigation is illustrated in Sec. 3 where it is shown that the antenna bandwidth is not reduced in the inductance, capacitance, and parallel-$LC$ cases, whereas it can be narrowed under specific conditions in the series-$LC$ case. Numerical examples confirming the theoretical analysis are provided in Sec. 4 and, finally, conclusions are drawn in Sec. 5.

## 2. BACKGROUND

The PRS-based LW antennas considered here are composed of a dielectric slab with relative permittivity $\varepsilon_r$, relative permeability $\mu_r = 1$, and thickness $h$, placed on a ground plane; at the air-dielectric interface we assume the presence of some screen (or structure) that partially shields the slab, i.e., a *partially-reflecting surface* (PRS) (see Fig. 1). A horizontal electric (or magnetic) dipole is assumed as a source, which is located at an height $z = h_s$ over the ground plane.

A transverse equivalent network (TEN) as in Fig. 2 is used to model such an antenna. In [12] and [6] it has been shown that a constant shunt susceptance $B_S$ is accurate for representing both superstrate dielectric layers and 2D periodic arrays of metal patches or slots placed on top of the grounded substrate; of course, the shunt susceptance varies with the angle of radiation, but for narrow-beam regions of interest (such as close to broadside) it may be assumed to be constant with $\theta$ and $\phi$.

The TEN model can be used either for the calculation of the far-field pattern radiated by a source through an application of the reciprocity theorem or for the determination of the wavenumber $k_\rho$ of a mode propagating along the structure in the $\rho$ direction [11].

In [11] it has been shown that when broadside radiation is considered, the main properties of the far field near the broadside direction are *equal* in the E and H planes. In particular, it has been shown that the radian frequency $\omega_{\text{opt}}$ at which the broadside power density is maximum is the one for which the following condition holds:

$$\cot(k_1 h) = \sqrt{\frac{1}{\varepsilon_r}}\,\eta_0 B_S \tag{1}$$

where $k_1 = \omega\sqrt{\varepsilon_r}/c$, $\eta_0$ is the free-space impedance, and $c$ is the speed of ligth in vacuum. Equation (1) requires the slab thickness $h$ to be approximately equal to one half of a wavelength inside the slab when the normalized susceptance $\bar{B}_S = B_S\eta_0$ is much larger than one (i.e., when the leaky parallel-plate waveguide is almost 'closed'); moreover, the source is optimally placed

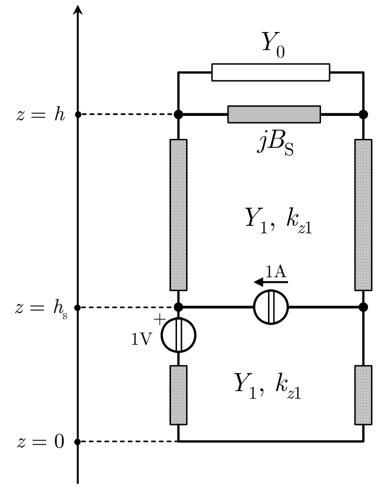


*Figure 2. Transverse equivalent network (TEN) for the structures in Fig. 1, excited by a unit-amplitude horizontal electric or magnetic dipole source (modeled by a parallel current source or a series voltage source, respectively).*

at $h_s = h/2$ or at $h_s = 0$ for an electric or a magnetic source, respectively. Condition (1) also implies the presence of a pair of dominant $\text{TE}_z$ and $\text{TM}_z$ LWs with small and nearly equal values of the phase constants and the attenuation constants [11] and can also be re-written as $B_{\text{in}} = 0$ where

$$B_{\text{in}} = B_S - Y_0 \cot(k_1 h) \tag{2}$$

is the input susceptance looking from above into the TEN model of the PRS structure and $Y_0 = 1/\eta_0$. It has been shown in [11] that for a frequency-independent susceptance an approximate closed-form formula can be obtained for the broadside pattern bandwith:

$$\text{BW} \simeq \frac{2\sqrt{\varepsilon_r}}{\pi}\,\frac{1}{\bar{B}_S^2} \tag{3}$$

## 3. FREQUENCY-DEPENDENT EQUIVALENT SUSCEPTANCES

In what follows we investigate how a *frequency-dependent* susceptance modelling the PRS would change the bandwidth performance of the considered antenna. Simple inductors or capacitors are considered as PRS transverse models, along with series- and parallel-$LC$ circuits, all shown in Fig. 3; these four cases are considered below.

### 3.1. Capacitor PRS

In the capacitor-PRS case, we can write

$$B_S(\omega) = B_{S_{\text{opt}}}\left(\frac{\omega}{\omega_{\text{opt}}}\right) \tag{4}$$

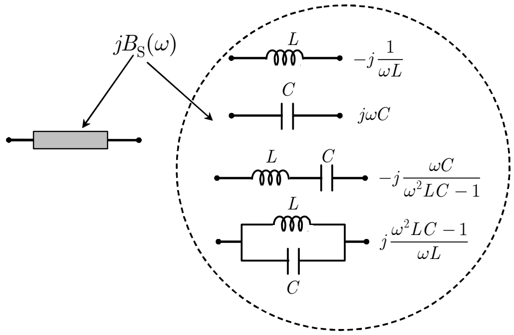


*Figure 3. Frequency-dependent susceptance models of the partially-reflecting surface.*

where $B_{\mathrm{S_{opt}}}$ is the value at the center frequency of operation $\omega_{\mathrm{opt}}$, at which the radiation at broadside is maximum. From (2) we can write

$$B_{\mathrm{in}} = B_{\mathrm{S_{opt}}}\left(\frac{\omega}{\omega_{\mathrm{opt}}}\right) - Y_0 \cot(k_1 h) \tag{5}$$

Near resonance, $k_1 h \simeq \pi$. Therefore, we can approximate the cotangent function in (5) using $\cot x \simeq 1/(x-\pi)$ (valid for $x \simeq \pi$). Normalizing the susceptance (multiplying by $\eta_0$), this yields

$$\bar{B}_{\mathrm{in}} = \bar{B}_{\mathrm{S_{opt}}}\left(\frac{\omega}{\omega_{\mathrm{opt}}}\right) + \frac{1}{\pi - k_1 h} \tag{6}$$

The derivative of the normalized input susceptance with respect to the frequency $\omega$ is

$$\frac{\partial \bar{B}_{\mathrm{in}}}{\partial \omega} = \frac{\bar{B}_{\mathrm{S_{opt}}}}{\omega_{\mathrm{opt}}} + \frac{h\sqrt{\varepsilon_{\mathrm{r}}}}{c\,(\pi - k_1 h)^2} \tag{7}$$

At the optimum frequency $\omega_{\mathrm{opt}}$ we have $\bar{B}_{\mathrm{in}} = 0$, and hence from (6)

$$\bar{B}_{\mathrm{in}} = \bar{B}_{\mathrm{S_{opt}}} + \frac{1}{\pi - k_{1\mathrm{opt}} h} = 0 \tag{8}$$

where $k_{1\mathrm{opt}}$ is the value of $k_1$ at the optimum frequency $\omega_{\mathrm{opt}}$. Therefore we can re-write the derivative above as

$$\left.\frac{\partial \bar{B}_{\mathrm{in}}}{\partial \omega}\right|_{\omega_{\mathrm{opt}}} = \frac{1}{\omega_{\mathrm{opt}}}\left[\bar{B}_{\mathrm{S_{opt}}} + (k_{1\mathrm{opt}} h)\,\bar{B}^2_{\mathrm{S_{opt}}}\right] \tag{9}$$

For a highly directive antenna, $\left|\bar{B}_{\mathrm{S_{opt}}}\right| \gg 1$; hence, the second term inside the square brackets in the above equation is much larger than the first term. This implies that the derivative is hardly affected by the frequency variation of the capacitor. Therefore, it follows that the bandwidth is limited by the frequency variation of the resonant (nearly half-wavelength) section of shorted transmission line in the TEN model, and not the capacitive PRS on top of it.

### 3.2. Inductor PRS

The inductor-PRS analysis is similar to the capacitor-PRS one, except that now we use

$$B_{\mathrm{S}}(\omega) = B_{\mathrm{S_{opt}}}\left(\frac{\omega_{\mathrm{opt}}}{\omega}\right) \tag{10}$$

Following the same steps as above, we easily obtain

$$\frac{\partial \bar{B}_{\mathrm{in}}}{\partial \omega} = -\frac{\bar{B}_{\mathrm{S_{opt}}}}{\omega}\frac{\omega_{\mathrm{opt}}}{\omega} + \frac{h\sqrt{\varepsilon_{\mathrm{r}}}}{c\,(\pi - k_1 h)^2} \tag{11}$$

Near resonance we can approximate (11) as

$$\frac{\partial \bar{B}_{\mathrm{in}}}{\partial \omega} = -\frac{\bar{B}_{\mathrm{S_{opt}}}}{\omega_{\mathrm{opt}}} + \frac{h\sqrt{\varepsilon_{\mathrm{r}}}}{c\,(\pi - k_1 h)^2} \tag{12}$$

so that

$$\left.\frac{\partial \bar{B}_{\mathrm{in}}}{\partial \omega}\right|_{\omega_{\mathrm{opt}}} = \frac{1}{\omega_{\mathrm{opt}}}\left[-\bar{B}_{\mathrm{S_{opt}}} + (k_{1\mathrm{opt}} h)\,\bar{B}^2_{\mathrm{S_{opt}}}\right] \tag{13}$$

Except for the minus sign in front of the first term, the result is the same as that for the capacitor, so the conclusion is the same. Therefore, the bandwidth for the inductor PRS is never significantly affected by the frequency variation of the PRS.

### 3.3. Series-LC PRS

In the series-$LC$ PRS case, we have

$$B_{\mathrm{in}} = -\left[\frac{\omega C}{\omega^2 LC - 1} + Y_0 \cot(k_1 h)\right] \tag{14}$$

Near the optimum frequency $\omega_{\mathrm{opt}}$ the cotangent function can be approximated as in the previous cases; moreover $1 - \omega^2 LC \simeq (1 - \omega\sqrt{LC}\,)(1 + \omega_{\mathrm{opt}}\sqrt{LC}\,)$, so that after some algebra (14) can be written as

$$\begin{aligned} B_{\mathrm{in}} \simeq &\left(\frac{Y_0}{\pi}\right)\left[\frac{1}{1 - \omega\left(\frac{h\sqrt{\varepsilon_{\mathrm{r}}}}{\pi c}\right)}\right] \\ &+ \left(\frac{\omega_{\mathrm{opt}} C}{1 + \omega_{\mathrm{opt}}\sqrt{LC}}\right)\left(\frac{1}{1 - \omega\sqrt{LC}}\right) \end{aligned} \tag{15}$$

This is of the form

$$B_{\mathrm{in}} \simeq \left(\frac{A_{\mathrm{TL}}}{1 - \omega/\omega_{\mathrm{TL}}}\right) + \left(\frac{A_{\mathrm{LC}}}{1 - \omega/\omega_{\mathrm{LC}}}\right) \tag{16}$$

where 'TL' denotes the transmission line and 'LC' denotes the $LC$ circuit. The frequency $\omega_{\mathrm{TL}}$ is the resonance frequency of the transmission line, at which $k_1 h = \pi$ (this is not the same as the frequency $\omega_{\mathrm{opt}}$, which is the frequency that gives the maximum power density at broadside). The frequency $\omega_{\mathrm{LC}} = 1/\sqrt{LC}$ is the resonance frequency of the series $LC$ circuit that models the

PRS. Note that both terms in the above equation, the one arising from the transmission-line resonator and the one arising from the $LC$ resonator, have the same form.

Taking the derivative, at the optimum frequency we have

$$\left.\frac{\partial B_{\text{in}}}{\partial \omega}\right|_{\omega_{\text{opt}}} \simeq \left[\frac{A_{\text{TL}}/\omega_{\text{TL}}}{\left(1-\omega_{\text{opt}}/\omega_{\text{TL}}\right)^2}\right]+\left[\frac{A_{\text{LC}}/\omega_{\text{LC}}}{\left(1-\omega_{\text{opt}}/\omega_{\text{LC}}\right)^2}\right] \tag{17}$$

Moreover, from (16), at $\omega_{\text{opt}}$ we also have

$$\left(\frac{A_{\text{TL}}}{1-\omega_{\text{opt}}/\omega_{\text{TL}}}\right)+\left(\frac{A_{\text{LC}}}{1-\omega_{\text{opt}}/\omega_{\text{LC}}}\right)=0 \tag{18}$$

Therefore, from (17) we obtain

$$\left.\frac{\partial B_{\text{in}}}{\partial \omega}\right|_{\omega_{\text{opt}}} \simeq \left(\frac{A_{\text{TL}}}{1-\omega_{\text{opt}}/\omega_{\text{TL}}}\right)\left[\frac{1}{\omega_{\text{TL}}-\omega_{\text{opt}}}-\frac{1}{\omega_{\text{LC}}-\omega_{\text{opt}}}\right] \tag{19}$$

The series $LC$-PRS will make a significant contribution to the derivative term (and hence be important in the determination of the bandwidth) if the second term inside the square brackets in (19) is significant relative to the first term.

Hence, the frequency variation of the PRS will not be important for the bandwidth, provided the transmission line is operating much closer to its resonance frequency than the PRS is.

That is, the frequency variation of the PRS will be unimportant for the bandwidth provided that $|\,\omega_{\text{TL}}-\omega_{\text{opt}}| \ll |\,\omega_{\text{LC}}-\omega_{\text{opt}}|$. The two resonance frequencies are related to each other. The closer we operate near the circuit resonance, the closer the $LC$ circuit will be to a short circuit. This, in turn, implies that the transmission line must then be operated closer to its resonance condition, in order to operate at the optimum point. Hence, it is not clear if the above condition will ever be satisfied, and if so, under what conditions. To explore this further, we invoke (1), which is satisfied at the optimum frequency $\omega_{\text{opt}}$. Approximating the cotangent function, and inserting the form of $B_{\text{S}}$ for the series $LC$ circuit, after some algebra we obtain

$$\frac{1-\omega\sqrt{LC}}{1-(k_1h/\pi)}=-\pi\frac{\eta_0}{\sqrt{\varepsilon_{\text{r}}}}\left(\frac{\omega C}{1+\omega\sqrt{LC}}\right) \tag{20}$$

This is approximately equivalent to

$$\frac{\omega-\omega_{\text{LC}}}{\omega-\omega_{\text{TL}}}=-\pi\frac{\eta_0}{\sqrt{\varepsilon_{\text{r}}}}\left(\frac{\omega C}{1+\omega\sqrt{LC}}\right) \tag{21}$$

which gives, taking into account that $\omega\sqrt{LC} \simeq \omega_{\text{LC}}\sqrt{LC} \simeq 1$:

$$\frac{\omega-\omega_{\text{LC}}}{\omega-\omega_{\text{TL}}}=-\pi\frac{\eta_0}{2\sqrt{\varepsilon_{\text{r}}}}\,\omega C \tag{22}$$

Therefore, a condition for the frequency variation of the series $LC$ circuit to be unimportant is

$$\pi\frac{\eta_0}{2\sqrt{\varepsilon_{\text{r}}}}\,\omega_{\text{opt}}C \gg 1 \tag{23}$$

That is

$$\bar{B}_C \gg \frac{2\sqrt{\varepsilon_{\text{r}}}}{\pi} \tag{24}$$

where $\bar{B}_C$ is the normalized susceptance of the capacitor in the series-$LC$ circuit.

### 3.4. Parallel-LC PRS

In the parallel-$LC$ PRS case, we have

$$B_{\text{in}}=-\left[\frac{1-\omega^2LC}{\omega L}+Y_0\cot\left(k_1h\right)\right] \tag{25}$$

Approximating the cotangent function, we obtain

$$B_{\text{in}} \simeq \frac{Y_0/\pi}{1-\omega\left(\frac{h\sqrt{\varepsilon_{\text{r}}}}{\pi c}\right)}-\frac{1}{\omega L}+\omega C \tag{26}$$

This has the form

$$B_{\text{in}} \simeq \left(\frac{A_{\text{TL}}}{1-\omega/\omega_{\text{TL}}}\right)+\left(\omega C-\frac{1}{\omega L}\right) \tag{27}$$

The derivative at the point of operation (maximum broadside radiation) is

$$\left.\frac{\partial B_{\text{in}}}{\partial \omega}\right|_{\omega_{\text{opt}}} \simeq \left(\frac{A_{\text{TL}}}{1-\omega_{\text{opt}}/\omega_{\text{TL}}}\right)\left(\frac{1}{\omega_{\text{TL}}-\omega_{\text{opt}}}\right)+\left(C+\frac{1}{\omega_{\text{opt}}^2L}\right) \tag{28}$$

Since at $\omega=\omega_{\text{opt}}$ we have $B_{\text{in}}=0$, from (27) and after some algebra, (28) can be re-written as

$$\left.\frac{\partial B_{\text{in}}}{\partial \omega}\right|_{\omega_{\text{opt}}} \simeq \left(\frac{A_{\text{TL}}/\omega_{\text{opt}}}{1-\omega_{\text{opt}}/\omega_{\text{TL}}}\right)\cdot\left[\frac{\omega_{\text{opt}}}{\omega_{\text{TL}}-\omega_{\text{opt}}}-\frac{1+\left(\omega_{\text{LC}}/\omega_{\text{opt}}\right)^2}{1-\left(\omega_{\text{LC}}/\omega_{\text{opt}}\right)^2}\right] \tag{29}$$

The second term inside the square brackets will be much smaller than the first term, provided the $LC$ circuit is not close to resonance. Note that for a PRS modeled as a parallel-$LC$ circuit, the circuit will not be operating near resonance for a highly-directive antenna (since the PRS should be close to a short circuit near the operating frequency, and not close to an open circuit). Hence, for a parallel-$LC$ PRS, the frequency variation of the $LC$ circuit is never of significant importance in the bandwidth calculation.

## 4. NUMERICAL RESULTS

In order to compare the frequency-dependent PRSs considered in the previous section, a reasonable way to proceed is to assume the same value for the magnitude of the normalized susceptance at the optimum frequency $\left|\bar{B}_{\mathrm{S}}(\omega_{\mathrm{opt}})\right| = \left|\bar{B}_{\mathrm{S_{opt}}}\right|$ for all the cases. It follows that for the simple capacitor and simple inductor cases we have

$$C = \frac{\left|\bar{B}_{\mathrm{S_{opt}}}\right|}{\eta_0\omega_{\mathrm{opt}}} \quad \text{and} \quad L = \frac{\eta_0}{\omega_{\mathrm{opt}}\left|\bar{B}_{\mathrm{S_{opt}}}\right|} \tag{30}$$

respectively. Note also that, maintaining the same optimum frequency $\omega_{\mathrm{opt}}$ for all the cases implies slightly different values of the optimum substrate thickness $h$, depending on the capacitive or inductive nature of the susceptance at the optimum frequency (see (1)).

As before, both in the parallel- and in the series-$LC$ circuits, we require to have the same fixed value of the normalized susceptance $\bar{B}_{\mathrm{S_{opt}}}$ at $\omega_{\mathrm{opt}}$ and, in addition, we choose the product $LC$ such that $LC = p/\omega_{\mathrm{opt}}^2$ (the parameter $p$ is a tuning parameter that indicates the separation between the LC resonance and the optimum frequency). Therefore, in the parallel case

$$C = \frac{\left|\bar{B}_{\mathrm{S_{opt}}}\right|}{\eta_0\omega_{\mathrm{opt}}}\,|p-1| \quad \text{and} \quad L = \frac{p}{|p-1|}\,\frac{\eta_0}{\omega_{\mathrm{opt}}\left|\bar{B}_{\mathrm{S_{opt}}}\right|} \tag{31}$$

while in the series case

$$L = \frac{\eta_0\,|p-1|}{\omega_{\mathrm{opt}}\left|\bar{B}_{\mathrm{S_{opt}}}\right|} \quad \text{and} \quad C = \frac{p\left|\bar{B}_{\mathrm{S_{opt}}}\right|}{|p-1|\,\omega_{\mathrm{opt}}\eta_0} \tag{32}$$

The inductive or the capacitive nature of the susceptance $\bar{B}_{\mathrm{S}}(\omega)$ depends on the value of $p$: If $\bar{B}_{\mathrm{S_{opt}}}$ is positive, $p$ should be chosen less than one for the series case, and larger than one for the parallel case.

For the structure considered in the numerical results, the excitation consists of an electric source placed in the middle of the slab. A relative permittivity $\varepsilon_{\mathrm{r}} = 2.2$ is assumed, while the optimum frequency and the absolute value of the normalized susceptance at the optimum frequency are chosen as $f_{\mathrm{opt}} = 20$ GHz and $\left|\bar{B}_{\mathrm{S_{opt}}}\right| = 20$, respectively. The value of the slab thickness $h$ is derived from (1) and is $h = 5.17$ mm for a capacitive susceptance and $h = 4.93$ mm for an inductive susceptance.

In Fig. 4(a), the broadside power density $P$ (in dB, relative to one Watt per steradian) is reported as a function of frequency for the cases of a simple capacitor and a simple inductor PRS. For comparison, also the corresponding cases that assume a frequency-independent value $\left|\bar{B}_{\mathrm{S}}(\omega)\right| = 20$ for the normalized susceptance are shown. In Fig. 4(b), the same as in (a) is reported for the cases of a parallel- and a series-$LC$ circuit. It has been assumed that $p = 2$, hence the parallel-$LC$ susceptance is capacitive and the series-$LC$ is inductive. For comparison, also in this figure the corresponding cases that assume a frequency-independent value $\left|\bar{B}_{\mathrm{S}}(\omega)\right| = 20$ for the normalized susceptance are shown.

From these figures, it can be observed that the frequency behavior of the PRS does not seem to be important in determining the bandwidth of the antenna.

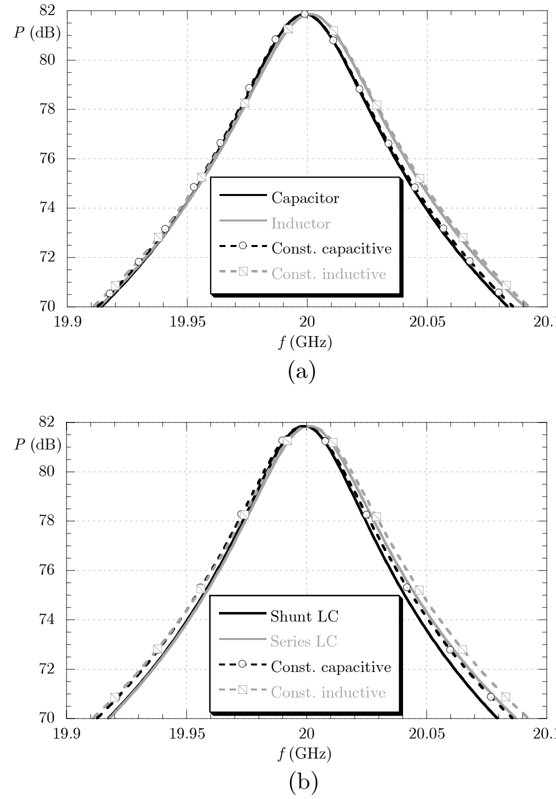


*Figure 4. Broadside power density $P$ as a function of frequency for a PRS-based antenna with $\varepsilon_r = 2.2$, $f_{opt} = 20$ GHz, and $\left|\bar{B}_{S_{opt}}\right| = 20$. (a) Simple capacitor and simple inductor PRS, together with the corresponding frequency-independent PRSs. (b) Parallel- and series-$LC$ PRS, together with the corresponding frequency-independent PRSs as in (a).*

In order to verify the conclusion about the possible effect of a series-$LC$ PRS on the bandwidth performance of the antenna, a comparison is presented between a structure with a frequency-independent PRS and a series-$LC$ PRS. Again, for a fair comparison, we assume that at the optimum frequency $\omega_{\mathrm{opt}}$ the values of the normalized susceptances are equal. Once the $C$ value has been fixed, the latter condition puts a constraint for the $L$ value of the $LC$ circuit. The capacitance $C$ is chosen according to

$$\eta_0\omega_{\mathrm{opt}}C = r_B\frac{2\sqrt{\varepsilon_{\mathrm{r}}}}{\pi} \tag{33}$$

as a function of $\omega_{\mathrm{opt}}$, $\varepsilon_{\mathrm{r}}$, and of the parameter $r_B$. According to the analysis in Sec. 3.3 (see (23)), when $r_B \gg 1$ we should not see a bandwidth variation in the series-$LC$ PRS structure with respect to the frequency-independent PRS one. For a structure with $f_{\mathrm{opt}} = 20$ GHz and $\left|\bar{B}_{\mathrm{S_{opt}}}\right| = 20$, in Fig. 5, the broadside power density $P$ is reported as a function of frequency for different cases: the frequency-independent PRS structure (*solid gray line*) and five series-$LC$ PRS structures with different values of $r_B$ (50, 10, 5, 2, and 1). It can thus be observed that, while for low values of $r_B$ the bandwidth performance is dramatically deteriorated, for $r_B \geq 10$,

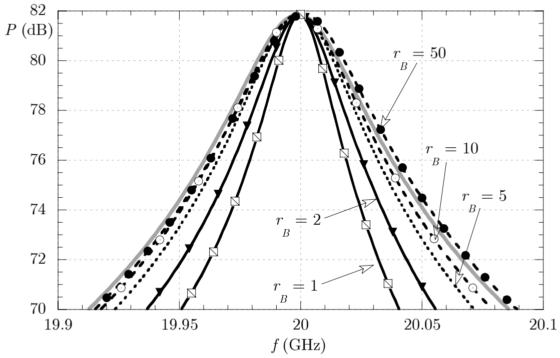


*Figure 5. Broadside power density $P$ as a function of frequency for a series-$LC$ PRS-based antenna with the same parameters as in Fig. 4, and different values of $r_B$, together with results for the corresponding frequency-independent PRS (solid gray line).*

the bandwidth behavior of the series-$LC$ PRS antenna is basically the same as the frequency-independent PRS one.

## 5. CONCLUSION

In this paper, the bandwidth properties of highly-directive planar leaky-wave antennas based on partially-reflecting surfaces have been studied. Assuming the possibility to describe the partially-reflecting surface with a shunt susceptance, it has been shown how the bandwidth of the antenna is affected by a frequency-dependent behavior of such susceptance. In particular, four kinds of partially-reflecting surfaces have been investigated, concluding that the frequency dependence is not important for the cases of a partially-reflecting surface modeled as $L$, $C$, or parallel-$LC$ elements; for a partially-reflecting surface modeled as a series-$LC$ element it may be important for some specific cases. It is also concluded that passive lossless realizations of the partially-reflecting surface cannot lead to bandwidth improvements with respect to the frequency-independent susceptance case, thus opening the investigation field to the consideration of lossy and/or active realizations.

## REFERENCES


[1] T. Tamir, *Leaky-Wave Antennas*, in R. E. Collin and F. J. Zucker (Eds.), *Antenna Theory*, New York: McGraw-Hill, 1969, Part 2, Ch. 20.

[2] A. A. Oliner, *Leaky-Wave Antennas*, in R. C. Johnson (Ed.), *Antenna Engineering Handbook*, New York: McGraw-Hill, 1993, Ch. 10.

[3] A. Ip and D. R. Jackson, "Radiation from cylindrical leaky waves," *IEEE Trans. Antennas Propagat.*, vol. 38, pp. 482–488, Apr. 1990.

[4] G. von Trentini, "Partially reflecting sheet arrays", *IEEE Trans. Antennas Propagat.*, vol. 4, 666-671, Oct. 1956.

[5] A. P. Feresidis and J. C. Vardaxoglou, "High gain planar antenna using optimised partially reflective surfaces," *IEE Proc. Microw. Antennas Propag.*, vol. 148, 345-350, Dec. 2001.

[6] T. Zhao, D. R. Jackson, J. T. Williams, and A. A. Oliner, "General formulas for 2D leaky-wave antennas," *IEEE Trans. Antennas Propagat.*, vol. 53, pp. 3525–3533, Nov. 2005.

[7] D. R. Jackson and A. A. Oliner, "A leaky-wave analysis of the high-gain printed antenna configuration," *IEEE Trans. Antennas Propagat.*, vol. 36, pp. 905–910, July 1988.

[8] D. R. Jackson, A. A. Oliner, and A. Ip, "Leaky-wave propagation and radiation for a narrow-beam multiple-layer dielectric structure," *IEEE Trans. Antennas Propagat.*, vol. AP–41, pp. 344–348, Mar. 1993.

[9] T. Zhao, D. R. Jackson, J. T. Williams, H.-Y. D. Yang, and A. A. Oliner, "2-D periodic leaky-wave antennas. Part I: Metal patch design," *IEEE Trans. Antennas Propagat.*, vol. 53, pp. 3505–3514, Nov. 2005.

[10] T. Zhao, D. R. Jackson, and J. T. Williams, "2-D periodic leaky-wave antennas. Part II: Slot design," *IEEE Trans. Antennas Propagat.*, vol. 53, pp. 3515–3524, Nov. 2005.

[11] G. Lovat, P. Burghignoli, and D. R. Jackson, "Fundamental properties and optimization of broadside radiation from uniform leaky-wave antennas," *IEEE Trans. Antennas Propagat.*, vol. 54, pp. 1442-1452, May 2006.

[12] T. Zhao, D. R. Jackson, J. T. Williams, and A. A. Oliner, "Simple CAD model for a dielectric leaky-wave antenna," *IEEE Antennas Wireless Propagat. Lett.*, vol. 3, pp. 243–245, 2004.

[13] R. E. Collin, *Foundations for microwave engineering*. 2nd ed. Hoboken, NJ: Wiley-IEEE Press, 2001.